Draft version October 4, 2021
Typeset using LaTeX default style in AASTeX63

Report

Kavli Summer Program in Astrophysics 2021

Looking for stellar magnetic activity cycles from photometric data

Samarth G. Kashyap
Tata Institute of Fundamental Research, Mumbai, India

Under the supervision of:
Savita Mathur
Instituto de Astrofisica de Canarias, Tenerife, Spain

Jérôme Ballot
Institut de Recherche en Astrophysique et Planétologie, France

In collaboration with:
Ângela R. G. Santos
University of Warwick, Coventry, UK

Rafael A. García
AIM, CEA, CNRS, Université Paris-Saclay, Université de Paris, France

ABSTRACT

Dark starspots on stellar surface results in brightness variability because of rotation and magnetic activity. In this study, we find candidates for the presence of magnetic activity cycles by analysing photometry data from *Kepler*. We use the standard deviation of the light curve (S_{ph}) as a proxy for magnetic activity and periodic/quasi-periodic variation of this measure is used to estimate the period of activity cycle. Using spot modelling, we conclude that the variation of photometric proxies of activity could also stem from long-lived features in a differentially rotating star. From a subsample of 5535 stars, we find 233 potential candidates with 63 of them suspected to be undergoing activity cycles and 170 of them suspected to have magnetic proxy variability due to differential rotation.

Keywords: Stellar activity – magnetic cycles – photometry

1. INTRODUCTION

Solar activity has been known to vary cyclically with a period of 11 years. It is also known that activity cycles are maintained by dynamo processes within the Sun. Although there is a broad consensus about the dynamo being the source of magnetic activity, understanding the detailed mechanism is an important question in solar physics (Charbonneau 2010). Along with the 11 year cycle, a 2-year quasi-periodicity has also been observed in the Sun over the years. Among the more comprehensive studies, Mursula et al. (2003) found such quasi-periodicity (of about 1.3 years) to exist over a period of 15 solar cycles. For the Sun, it is also well known that the helioseismic mode frequencies increase and their amplitudes decrease with increase in magnetic activity (e.g., Woodard & Noyes 1985; Bachmann & Brown 1993; Chaplin et al. 2007). The Sun being a main-sequence star, a study of stellar magnetic activity would provide a broader context for the activity cycle of the Sun.

Leighton (1959) found that Ca II H and K emission lines were more intense in areas of concentrated magnetic fields. Subsequently several surveys were led to study chromospheric activity of stars (e.g., Wilson 1978; Hall et al. 2007). Wilson (1978) observed chromospheric activity in both the Sun as well as Sun-like stars and concluded that the cyclic nature of H and K fluxes was evidence for stellar magnetic cycles. Vaughan & Preston (1980) studied F-G-K-M stars and found that most of the observed stars showed either high or low chromospheric activity but very few exhibited

intermediate activity – what is today known as the Vaughan-Preston gap. While the literature on chromospheric activity measurement kept building up, Baliunas & Vaughan (1985) studied solar luminosity variations over a sunspot cycle and also found long term luminosity fluctuations in chromospherically active stars, thus establishing a link between photometric variation and chromospheric activity. Lockwood et al. (2007) studied photometric variation of 32 stars along with chromospheric activity variation and found a correlation between brightness and Ca II emission for older (less active) stars and anti-correlation for younger stars. More recently, Santos et al. (2019) measured photometric activity and surface rotation rates for ∼15,000 M and K main-sequence stars from *Kepler*.

It is known that astroseismic oscillations are affected by magnetic activity. Using data from CoRoT (Convection, Rotation and planetary Transits; Baglin et al. 2006), García et al. (2010) observed that both astroseismic mode frequencies and amplitudes of HD49933 revealed a modulation of at least 120 days, with the frequency shift minima corresponding to amplitude maxima - a behaviour which is seen in the Sun; the magnetic activity of HD49933 was also confirmed using Ca H and K lines. This star was further studied by Salabert et al. (2011), who observed larger frequency shifts for high-frequency modes, who suggested that this indicated a change in magnetic activity in outer layers of the star. Fletcher et al. (2010) observed characteristics of quasi-biennial variation of the helioseismic p-mode frequencies. Salabert et al. (2016) found that the low-degree seismic mode frequencies of solar analog KIC 10644253 have a temporal variability modulation of about 1.5 years, which was suggested to be due to physical mechanisms in the inner subsurface layers.

Baliunas et al. (1996) found a relation between activity cycle period (P_{cyc}) and rotation period (P_{rot}) to follow a power law in dynamo number D, an important parameter in stellar dynamo models. Brandenburg et al. (1998) also studied "period-ratio" (PR), P_{cyc}/P_{rot}, and suggested that in the course of stellar evolution, there is a jump in the PR value by a factor of ~ 6 near the Vaughan-Preston gap, thus indicating the PR to be an indicator of high/low activity. Oláh & Strassmeier (2002) found a correlation between P_{cyc} and P_{rot} for fast rotating active binaries. Böhm-Vitense (2007) studied main-sequence G and K stars and found that P_{cyc} increases with P_{rot}. They found that these stars lie on two distinct branches, an "active" branch with relatively faster rotating stars and an "inactive" branch with cooler and slower rotating stars and hypothesised the operation of two different kinds of dynamos. Figure (1) shows the active and inactive branches recognized by Böhm-Vitense (2007).

It is in this backdrop that the current study is motivated. Equipped with a catalog of $\sim$ 55,000 stars with measured rotation periods from the NASA *Kepler* mission (Santos et al. 2019, 2021), a more definitve relationship between P_{cyc} and P_{rot} is sought. The organisation of this report is as follows. In Section (2), we discuss the observational data used and data selection procedure. Subsequently, we discuss the data analysis procedure in Section (3) and validation of the method used in Section (3.1). The validity of the method used to find magnetic activity cycles is mooted in Section (4) and the results are discussed in Section (5).

2. OBSERVATIONS AND DATA SELECTION

The *Kepler* mission sought to detect Earth-like planets near the habitable zones of Sun-like stars (Borucki et al. 2010). The mission collected photometry data of $\sim 156,000$ stellar targets continuously for ~ 3.5 years, with a cadence of 29.4 min, called as the Long Cadence (LC) dataset (Jenkins et al. 2010). A subset of these stellar targets are also observed at a shorter cadence of 1 minute intervals for their astroseismic characterization (Gilliland et al. 2010). For the present study, the LC dataset is used as we are interested in the long term variability. The stellar targets are recognized with their Kepler Input Catalog (KIC) numbers and the photometry dataset is publicly available (Thompson et al. 2016) on the Mikulski Archive for Space Telescopes[1].

The *Kepler* dataset is divided in 17 observational quarters[2], with each quarter lasting about 90 days. The spacecraft rolls 90° at the end of each quarter, such that the solar-arrays are pointed towards the Sun and the radiators which cool the Focal Plane Array (FPA) are pointed away from the Sun (Haas et al. 2010). This also results in the stellar targets to be rotated on to new detectors in the FPA. Hence, the dataset corresponding to each of the quarterly segments are calibrated independently. The variability introduced by differences in calibration can be thought as multiplying the "true" signal with a window-function which is constant within a quarterly segment but varies across segments. This results in a yearly periodic variability, in some stellar targets.

We use the catalog by Santos et al. (2021), who determined rotation period of $\sim$ 55,000 stars observed by *Kepler*. Differential rotation results in conversion of poloidal magnetic field to a toroidal magnetic field. Hence, faster rotation

[1] MAST
[2] github.com/barentsen/kepler-skye/kepler-quarters.csv

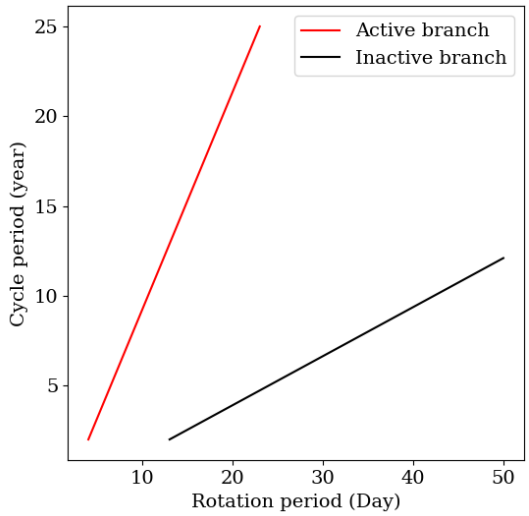

Figure 1. The plot of P_{rot} vs P_{cyc} adapted from Böhm-Vitense (2007). The red line shows the active branch and the black line shows the inactive branch. The Sun lies on neither of the branches.

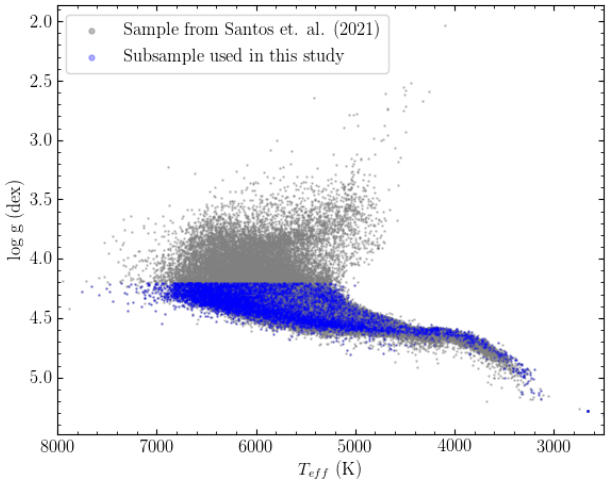

Figure 2. H-R diagram showing sample of stars with measured rotation periods (Santos et al. 2021) in gray and the sample of stars studied in this work to search magnetic activity cycles in blue.

implies that the star has a shorter activity cycle. This can also be seen in the active-branch in Figure (1) – the fastest rotators have the shortest cycle periods. Since the *Kepler* dataset spans 4 years, we are more likely to observe a full cycle, if fast rotators are studied. For the current analysis, we have looked at stars with $P_{rot} < 20$ days, with a special focus on fast rotators i.e $P_{rot} < 10$ days. Excluding sub-giants and potential binary candidates, the subsample has 5535 stars.

3. DATA ANALYSIS

Magnetic activity on stars result in dark starspots. The number and size of spots depends on the strength of stellar magnetic activity. The motion of these spots on the stellar disk results in variation in brightness. Hence the brightness variation encodes the information of rotation and activity of a star. The light-curve is modulated with the rotation period and activity results in the modulation of the light-curve envelope. Hence a measure of the width of the light-curve envelope can indicate the level of magnetic activity. García et al. (2010) first used the standard deviation of the stellar light-curve as a proxy for magnetic activity. This proxy, applied to overlapping segments of light-curve was used by Mathur et al. (2014) as a proxy for the variation of stellar magnetic activity. The standard deviation of the light-curve segment is called S_{ph} and each segment is taken to have a width of $5 \times P_{rot}$, where P_{rot} is the rotation period of the star. This measurement was subsequently validated by Salabert et al. (2017) through the determination of the solar activity cycle period (11 year and quasi-biennial variation) using data from Variability of Solar Irradiance and Gravity Oscillations (VIRGO; Fröhlich et al. (1995)) and Global Oscillations at Low Frequency (GOLF; Gabriel et al. (1995)). They found that S_{ph} has a Spearman's correlation coefficient of more than 0.85 with other magnetic proxies such as total sunspot number, total sunspot area, 10.7 cm radio flux, Ca II K-line emission index and astroseismic frequency shifts. The present study uses the S_{ph} measurement on a subset of *Kepler* LC targets. The data analysis procedure to search for magnetic activity variability or cycles, consists of the following steps:

1. Computation of the S_{ph} with a window of $5 \times P_{rot}$.
2. Computation of Fourier transform of the light-curve, $D(\omega)$.
3. Computation of Fourier transform of $S_{ph}(t)$, $S(\omega)$.

The variation of S_{ph} is fitted with a sine-curve as follows:

$$S(t) = A \sin\left(\frac{2\pi t}{T} + \beta\right) \tag{1}$$

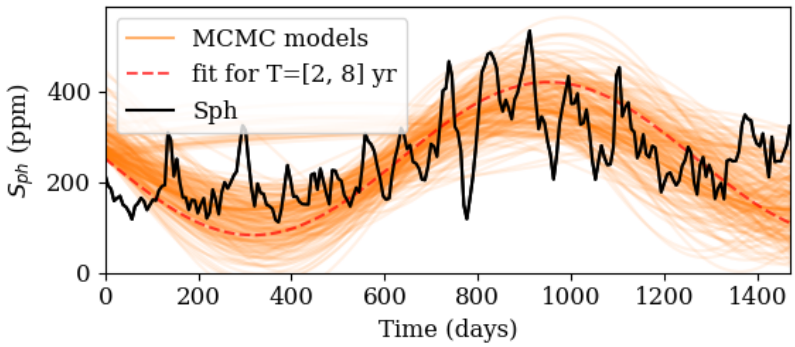

Figure 3. S_{ph} for KIC 3733735 is shown as a black line. Best sine-curve fit using least square fitting is shown in a red-dotted line (fit period = 3.47 years) and some MCMC samples are shown using orange lines (estimated period = 3.29 ± 0.39 years).

where A is the amplitude, T is the characteristic time period and β is the phase. The fitting procedure involves estimation of (A, T, β) and the optimal solution is when $T = P_{cyc}$. The S_{ph} is normalized for ease of fitting and the bounds for each of the parameters are given below:

$$\begin{aligned} 0 \leq A \leq 2 \\ 2 \text{ years} \leq T \leq 8 \text{ years} \\ 0 \leq \beta \leq 2\pi \end{aligned} \tag{2}$$

The parameter estimation is performed using two different methods: least square fitting and Bayesian estimation using Markov Chain Monte Carlo method (MCMC). MCMC estimation is performed using flat priors which are non-zero in the ranges given in Equation (2). The Bayesian estimation was performed using `emcee` (Foreman-Mackey et al. 2013).

3.1. *Validation of methodology - VIRGO*

We use solar irradiance data from VIRGO to validate the methodology of activity cycle period estimation. The VIRGO data is recorded at a cadence of 1 minute for a total duration of 25 years. We compute the S_{ph} for this time-series and we fit a sine-curve to estimate the periodicity of activity cycle. Figure (4) shows such a fitting performed on S_{ph} computed on the RED-channel of VIRGO. The fitted P_{cyc} is found to be 12.03 ± 0.33 years, which is in reasonable agreement with established literature. We do perform fitting for the BLUE and GREEN channels as well and the fitted P_{cyc} is found to be robust across channels. However, it is to be noted that, in this case, the time-series captures data for 2 full magnetic cycles. Does this procedure work well even if only a part of the cycle is observed? To address this, we artificially create *Kepler*-like data from the existing time-series by binning and windowing. We first bin the dataset to 30 minutes. In the case of VIRGO, there are instances of missing data scattered throughout the entire period of 25 years. Hence, the following gap filling procedure is employed in such a way that the S_{ph} computation isn't hampered.

1. When missing data-point is encountered, 10 neighbouring points are considered on either side of point. If none of these are missing, then a cubic interpolation is performed to fill the missing data.

2. If missing data points are found in the 10-neighbour vicinity, then these are treated as clusters of missing data and hence will not be considered for the S_{ph} computation.

Hence the minimal gap filling performed does not change the masurement of S_{ph} itself. This 25-year long rebinned data is then windowed with a window length of 4 years. The 4-year window is then moved by 1 month to create a new segment. There are 307 such segments. Each of these segments act as *Kepler*-like observations of the Sun at different levels of magnetic activity. Figure (5) shows an estimation of magnetic cycle periods from the *Kepler*-like segments of VIRGO data. The uncertainities in the inference is about ±2.5 years. It can be seen that the period underestimation is severe in near the minima of solar activity. In other regions, the estimated period is found to be roughly 7 ± 2.5 years, which is still an underestimate for the 11 year cycle period of the Sun. This is expected, as we are observing the Sun for a fraction of the entire cycle. We emphasize that, while the fitting procedure works when

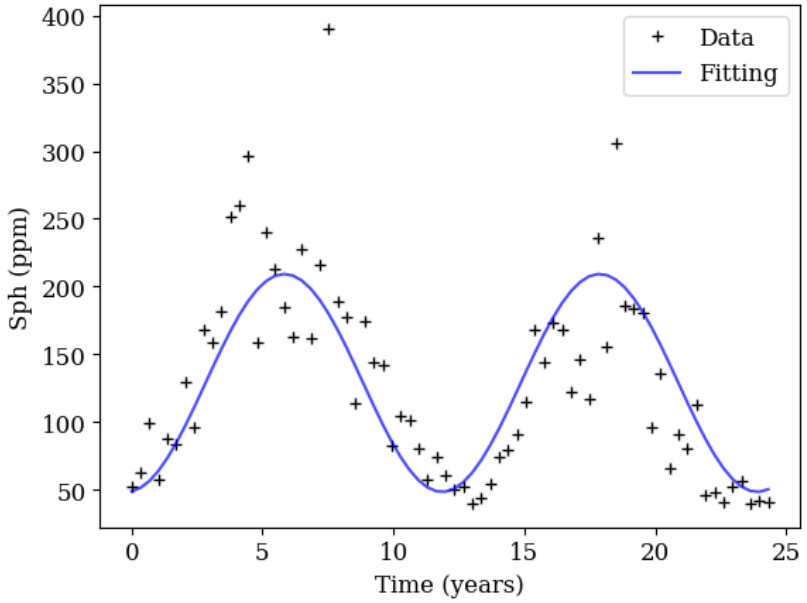

Figure 4. The S_{ph} computed from VIRGO solar photometry data (RED channel) is shown (+) along with the sine-curve fit (blue). The fit period is found to be 12.03 ± 0.33 years.

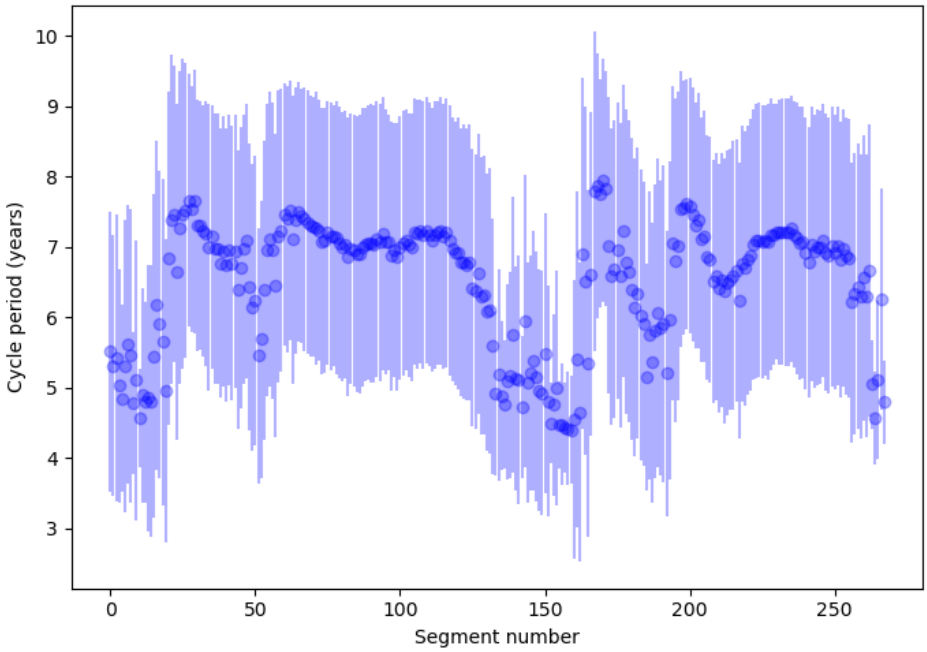

Figure 5. Estimation of solar activity cycle period from each of the *Kepler*-like segments of VIRGO data. In the regions of low solar activity (near segments 1 and segment 150), it can be seen that the estimation is more erroneous.

the data for the entire cycle is present, there is an underestimate of the P_{cyc} when only a part of the cycle is observed. The underestimation becomes severe when the observation is near the minima of magnetic activity. Hence, we expect the method to perform better for stars which have completed entire cycles or most of the cycle within the observation period of *Kepler* i.e. 4 years.

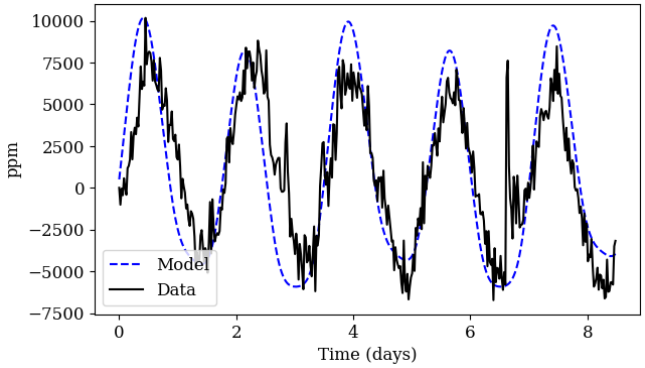

Figure 6. Two-spot model for KIC 2300039. The observed light curve is shown in blue and the model is shown in orange. It can be seen that the model captures the broad features of the lightcurve. The spikes in the data at ~ 3 days and ~ 6.5 days is possibly due to flaring, which is not part of the model.

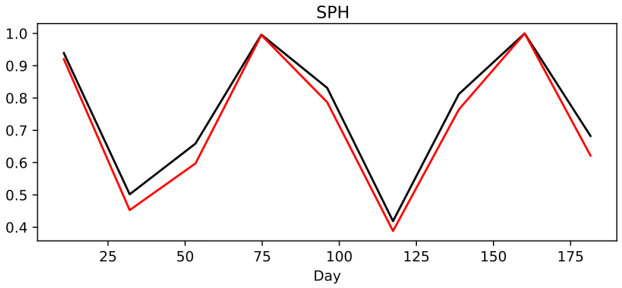

Figure 7. S_{ph} computed for two different synthetic light-curves. The black line corresponds to S_{ph} (normalized) computed for a stellar model with differential rotation. The red line corresponds to S_{ph} (normalized) corresponding to constant rotation and variable magnetic activity.

4. DOES VARIABILITY OF PHOTOMETRIC PROXY FOR ACTIVITY IMPLY STELLAR ACTIVITY CYCLE?

While brightness variation has been linked to magnetic activity, we note that variation in S_{ph} (or other photometric proxies of activity) could be due to factors other than magnetic activity variation. Most notably, it has been known that long-lived structures create a beating pattern in the light-curves (e. g., KIC 3733735, nicknamed Shere Khan, KIC 9226926; Mathur et al. 2014). We employ the use of simplistic models to study if effects other than activity cycle could lead to periodic variation of S_{ph}. The starspot simulation code developed by Santos et al. (2017) was modified to simulate a star with two active regions located at different latitudes. The model considers the following variable parameters.

1. Latitude, longitude and areas of active regions (θ, ϕ, A).
2. Differential rotation, $\Omega(\theta)$, and active region lifetime, τ.
3. Limb darkening and inclination angle of rotation axis with the observer's line of sight, α.

Since beating effect was seen due to long-lived features, these spots were treated to be infinitely-lived and have a fixed size. Before proceeding to construct synthetic light-curve, we first construct the light curve of a chosen *Kepler* target (KIC 2300039) and establish that the model could reproduce observed light curves. Figure (6) shows that the model reproduces the observed light-curve reasonably well.

We now construct light curves for two different scenario; (a) light-curve is modulated by differential rotation and (b) magnetic activity cycle results in light-curve variability. By adjusting parameters $(A, \Omega(\theta))$, we could construct light-curves which exhibit almost identical variation in S_{ph}. Figure (7) shows S_{ph} variation for two cases.

1. Differentially rotating star with 2 active regions present at different latitudes.
2. Star undergoing solid-body rotation, but varying magnetic activity over time.

As it can be seen from Figure (7), the variation of S_{ph} could either be due to magnetic activity changes or because of beating due to long-lived structures. We note that this holds not just for the measurement of S_{ph} but other photometric proxies as well.

5. RESULTS AND DISCUSSION

We estimate the period of the observed variability in the fast rotators ($P_{rot} < 10$ days) from the rotation catalog of Santos et al. (2021). This results in 5535 targets for which the analysis is carried out. Although the fitting procedure provides a solution to every single stellar target, we perform visual checks to establish the following:

- Fitting captures the long-term variation in S_{ph} reasonably well.

Table 1. Candidates for activity cycle. The *Kepler* KIC is listed along with P_{rot} estimated from fitting and MCMC.

KIC	P_{cyc} fitted	P_{cyc} from MCMC
3336651	3.45	3.46 ± 0.30
3336651	3.45	3.46 ± 0.31
4148847	3.66	5.33 ± 2.25
4826451	2.22	2.79 ± 0.53
4833652	3.97	3.69 ± 0.86
4861784	3.52	6.26 ± 2.46
5033359	3.88	2.10 ± 0.58
5184732	4.42	4.47 ± 1.21
5184732	4.42	4.46 ± 1.22
5268904	3.25	3.25 ± 3.01
5309966	3.96	3.85 ± 1.23
5309966	3.96	3.81 ± 1.10
5807484	3.12	3.74 ± 2.14
5965012	4.58	4.39 ± 0.95
6037036	8.00	7.02 ± 1.97
6058858	3.15	5.16 ± 2.95
6277018	8.00	2.79 ± 2.54
6356144	6.01	3.00 ± 2.46
6445537	5.03	4.45 ± 1.68
6521526	3.75	3.76 ± 0.59
6542087	4.07	4.75 ± 1.75
6590179	4.36	4.72 ± 1.59
6630715	8.00	2.50 ± 2.19
6688223	4.42	5.76 ± 2.15
6763067	5.43	5.98 ± 3.08
6782577	4.44	5.57 ± 1.94
6870760	4.31	6.23 ± 2.16
6888300	3.56	4.25 ± 1.35
6949412	3.38	3.43 ± 0.14
6953069	2.56	2.57 ± 0.05
7035942	4.75	4.78 ± 1.65
7117293	4.62	5.11 ± 1.85

KIC	P_{cyc} fitted	P_{cyc} from MCMC
7352862	3.35	3.38 ± 0.51
7354297	5.28	5.30 ± 2.46
7378049	5.00	6.05 ± 2.00
7379772	3.31	3.38 ± 0.47
7422811	6.40	2.71 ± 0.29
7428892	5.09	6.32 ± 1.95
7503882	8.00	4.15 ± 2.87
7870112	3.18	5.39 ± 2.38
7870112	3.18	5.42 ± 2.38
7871531	3.45	3.38 ± 2.24
7871531	3.45	3.41 ± 2.34
7970740	3.54	3.57 ± 2.56
7970740	3.54	3.54 ± 2.37
8677016	2.21	3.97 ± 2.66
8677016	2.21	3.94 ± 2.68
8696343	4.07	3.89 ± 1.03
8696343	4.07	3.88 ± 1.05
8776961	2.76	3.33 ± 2.66
8776961	2.76	3.34 ± 2.71
9206432	8.00	7.35 ± 1.95
9206432	8.00	7.31 ± 1.95
9226926	5.06	4.61 ± 0.75
9226926	5.06	4.61 ± 0.74
10794845	5.92	6.66 ± 1.43
10794845	5.92	6.68 ± 1.45
11070918	2.60	8.73 ± 1.40
11070918	2.60	8.73 ± 1.41
12069127	1.88	2.16 ± 0.47
12069127	1.88	2.16 ± 0.50
12735580	4.69	6.41 ± 2.02
12735580	4.69	6.45 ± 2.01

- The long-term variation is not due to instrumental effects (such as the quarterly variation of *Kepler*).
- Classify whether the targets are more likely candidates with beating or candidates for activity cycles.

From this analysis, we find 63 stellar targets which are candidates for activity cycles. The list of candidates are listed in Table (1) along with their estimated variability periods. These candidates are chosen because of the similarity of the S_{ph} variation to that of Shere-Khan. A spectroscopic follow-up study of these candidates would help establish the presence of cycles in these stars. For the sake of demonstration, the analysis of a few candidates is shown in Appendix (A).

We also find 170 candidates where it is suspected that the S_{ph} variation is due to beating of closely spaced frequencies. However, the classification of cycle/beating would only be confirmed through the study of chromospheric activity from spectroscopy. To understand the activity-rotation period relation, we plot P_{cyc} against P_{rot} in Figure (8). Among the fast rotators, it is inconclusive whether the candidates for activity lie on the "active" branch. The high degree of scatter prevents making a definitive conclusion regarding the relation between P_{cyc} and P_{rot}. There is some concentration of points near $P_{cyc} = 8$. This is due to the fact the solution reaching the maximum allowable period in the period search algorithm. As seen in Section (3.1), these numbers are more likely underestiming the actual cycle period.

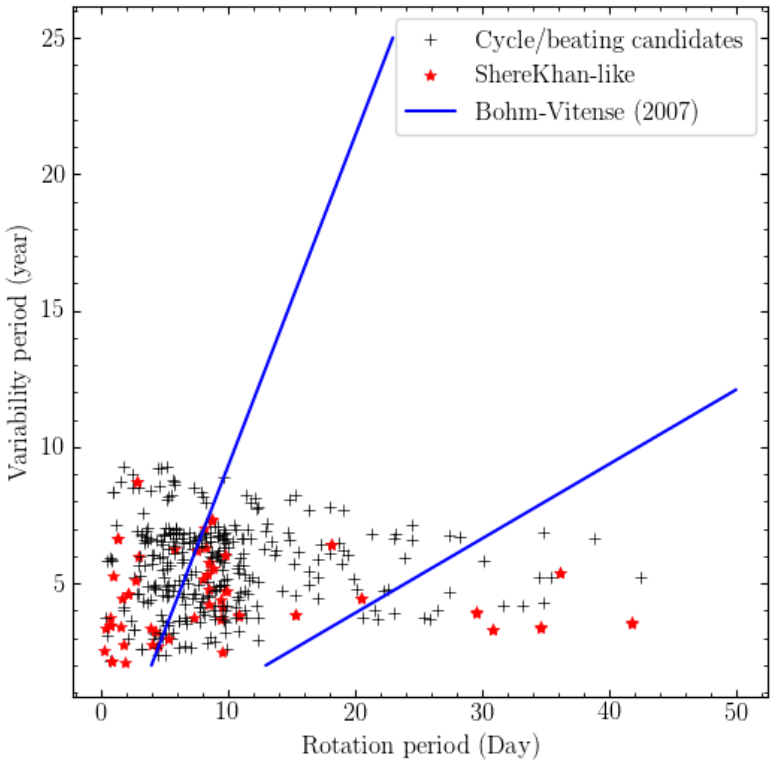

Figure 8. The estimated variability period is plotted against the rotation period of the stars. The blue lines indicate the "active" and "inactive" branches as identified by Böhm-Vitense (2007). The candidates for activity cycles (red *) and beating (+) are also shown.

Another parameter of interest is the Rossby number, which is the ratio of rotation period to the convective turnover time. This parameter is useful for a comparison of stars with different convective envelopes and is an important quantity in dynamo models. The Rossby numbers are computed based on the formula by (Noyes et al. 1984). Figure (9) shows the relation between Rossby number and the mean S_{ph}. The mean S_{ph} is an indicator of magnetic activity. For Rossby numbers in the range of $(0.1, 1)$, it is seen that stronger magnetic activity is observed in stars with smaller Rossby numbers. The activity proxy also saturates at around 2×10^4. No correlation is seen between the variability period and the Rossby number. While the current method can be used to estimate the periodicity of variability in the S_{ph}, complementary spectroscopic observations would be needed to establish the presence of an activity cycle. The subsample used also has 9 candidates with astroseismic detection and a closer analysis of the astroseismic data is necessary to confirm the existence of activity cycles.

REFERENCES

Bachmann, K. T., & Brown, T. M. 1993, ApJL, 411, L45, doi: 10.1086/186908

Baglin, A., Auvergne, M., Boisnard, L., et al. 2006, in 36th COSPAR Scientific Assembly, Vol. 36, 3749

Baliunas, S. L., Nesme-Ribes, E., Sokoloff, D., & Soon, W. H. 1996, ApJ, 460, 848, doi: 10.1086/177014

Baliunas, S. L., & Vaughan, A. H. 1985, ARA&A, 23, 379, doi: 10.1146/annurev.aa.23.090185.002115

Böhm-Vitense, E. 2007, ApJ, 657, 486, doi: 10.1086/510482

Borucki, W. J., Koch, D., Basri, G., et al. 2010, Science, 327, 977, doi: 10.1126/science.1185402

Brandenburg, A., Saar, S. H., & Turpin, C. R. 1998, ApJL, 498, L51, doi: 10.1086/311297

Chaplin, W. J., Elsworth, Y., Miller, B. A., Verner, G. A., & New, R. 2007, ApJ, 659, 1749, doi: 10.1086/512543

Charbonneau, P. 2010, Living Reviews in Solar Physics, 7, 3, doi: 10.12942/lrsp-2010-3

Fletcher, S. T., Broomhall, A.-M., Salabert, D., et al. 2010, ApJL, 718, L19, doi: 10.1088/2041-8205/718/1/L19

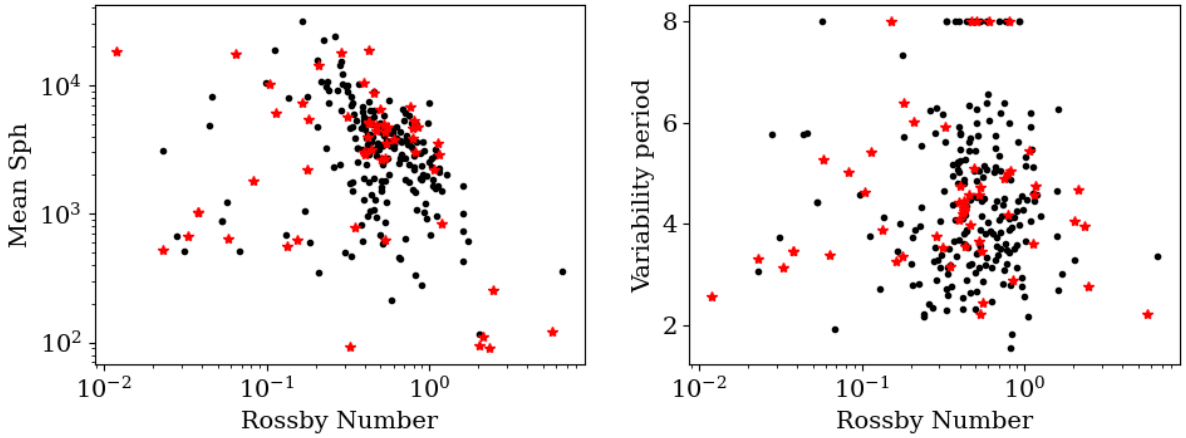

Figure 9. Rossby number plotted against the mean S_{ph} and variability periods. The red points correspond to Shere Khan-like candidates and the black points show candidates for beating.

Foreman-Mackey, D., Hogg, D. W., Lang, D., & Goodman, J. 2013, PASP, 125, 306, doi: 10.1086/670067

Fröhlich, C., Romero, J., Roth, H., et al. 1995, SoPh, 162, 101, doi: 10.1007/BF00733428

Gabriel, A. H., Grec, G., Charra, J., et al. 1995, SoPh, 162, 61, doi: 10.1007/BF00733427

García, R. A., Mathur, S., Salabert, D., et al. 2010, Science, 329, 1032, doi: 10.1126/science.1191064

Gilliland, R. L., Jenkins, J. M., Borucki, W. J., et al. 2010, ApJL, 713, L160, doi: 10.1088/2041-8205/713/2/L160

Haas, M. R., Batalha, N. M., Bryson, S. T., et al. 2010, ApJL, 713, L115, doi: 10.1088/2041-8205/713/2/L115

Hall, J. C., Lockwood, G. W., & Skiff, B. A. 2007, AJ, 133, 862, doi: 10.1086/510356

Jenkins, J. M., Caldwell, D. A., Chandrasekaran, H., et al. 2010, ApJL, 713, L120, doi: 10.1088/2041-8205/713/2/L120

Leighton, R. B. 1959, ApJ, 130, 366, doi: 10.1086/146727

Lockwood, G. W., Skiff, B. A., Henry, G. W., et al. 2007, ApJS, 171, 260, doi: 10.1086/516752

Mathur, S., García, R. A., Ballot, J., et al. 2014, A&A, 562, A124, doi: 10.1051/0004-6361/201322707

Mursula, K., Zieger, B., & Vilppola, J. H. 2003, SoPh, 212, 201, doi: 10.1023/A:1022980029618

Noyes, R. W., Hartmann, L. W., Baliunas, S. L., Duncan, D. K., & Vaughan, A. H. 1984, ApJ, 279, 763, doi: 10.1086/161945

Oláh, K., & Strassmeier, K. G. 2002, Astronomische Nachrichten, 323, 361, doi: 10.1002/1521-3994(200208)323:3/4361::AID-ASNA3613.0.CO;2-1

Salabert, D., García, R. A., Jiménez, A., et al. 2017, A&A, 608, A87, doi: 10.1051/0004-6361/201731560

Salabert, D., Régulo, C., Ballot, J., García, R. A., & Mathur, S. 2011, A&A, 530, A127, doi: 10.1051/0004-6361/201116633

Salabert, D., Régulo, C., García, R. A., et al. 2016, A&A, 589, A118, doi: 10.1051/0004-6361/201527978

Santos, A. R. G., Breton, S. N., Mathur, S., & García, R. A. 2021, ApJS, 255, 17, doi: 10.3847/1538-4365/ac033f

Santos, A. R. G., Cunha, M. S., Avelino, P. P., García, R. A., & Mathur, S. 2017, A&A, 599, A1, doi: 10.1051/0004-6361/201629923

Santos, A. R. G., García, R. A., Mathur, S., et al. 2019, ApJS, 244, 21, doi: 10.3847/1538-4365/ab3b56

Thompson, S. E., Fraquelli, D., Van Cleve, J. E., & Caldwell, D. A. 2016, Kepler Archive Manual, Kepler Science Document KDMC-10008-006

Vaughan, A. H., & Preston, G. W. 1980, PASP, 92, 385, doi: 10.1086/130683

Wilson, O. C. 1978, ApJ, 226, 379, doi: 10.1086/156618

Woodard, M. F., & Noyes, R. W. 1985, Nature, 318, 449, doi: 10.1038/318449a0

APPENDIX

A. CANDIDATES

In the plots below, we demonstrate the analysis method used. In the Figures (10-13), the top-left panel shows the light-curve, with the *Kepler* quarters marked with blue vertical lines. These help us to visually identify the presence of calibration artefacts. The top-right panel shows the S_{ph} computed from the light curve. The bottom panels show the Fourier transform of the time-domain counterparts in the top panels.

- Figure (10) shows KIC 3733735, which has been previously known for existence of activity cycle. The Fourier transform of the light-curve has a very dominant single peak which hints that the variation in S_{ph} could be due to changes in magnetic activity.
- Figure (11) shows KIC 4826451, which is another example of periodic variation of S_{ph} with single dominant peak observed in the light-curve (Fourier domain).
- Figure (12) shows KIC 7506027, which has multiple peaks in the Fourier transform of the light curve. The estimates variability period (~ 2 years) is one of the beating frequencies from the multiple peaks.
- Figure (13) shows KIC 3236788. It does have multiple peaks in the Fourier transform of the light-curve, but the secondary peaks are not as strong as the primary peak. Hence, it is suspected that this target is exhibits a combination of beating with changes in activity.

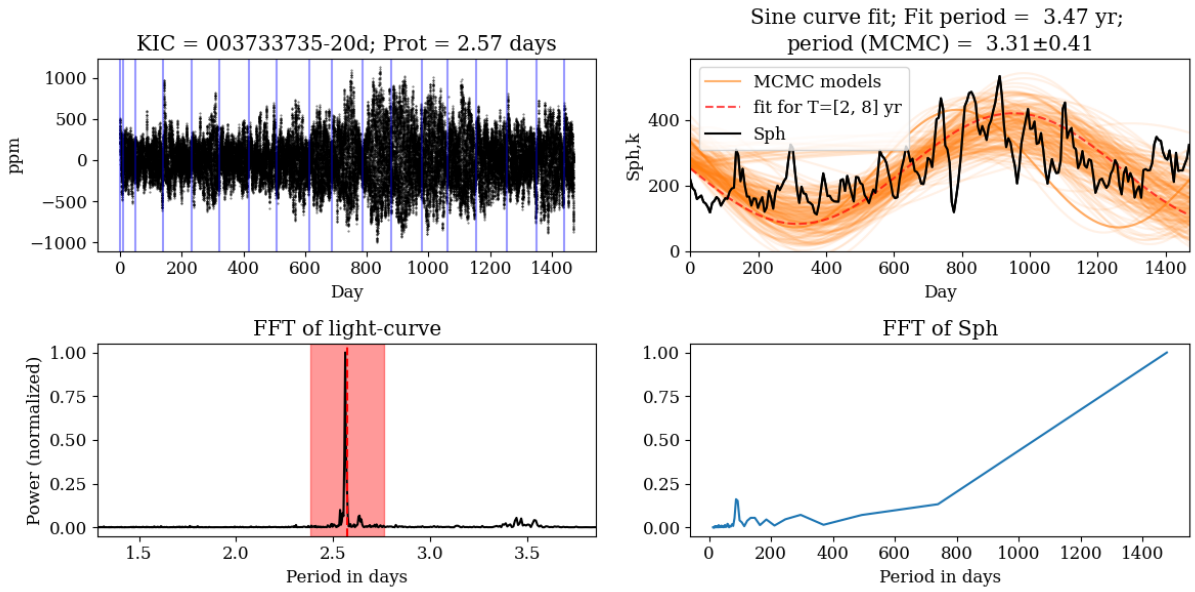

Figure 10. KIC 3733735 (Shere Khan). Candidate for activity cycle.

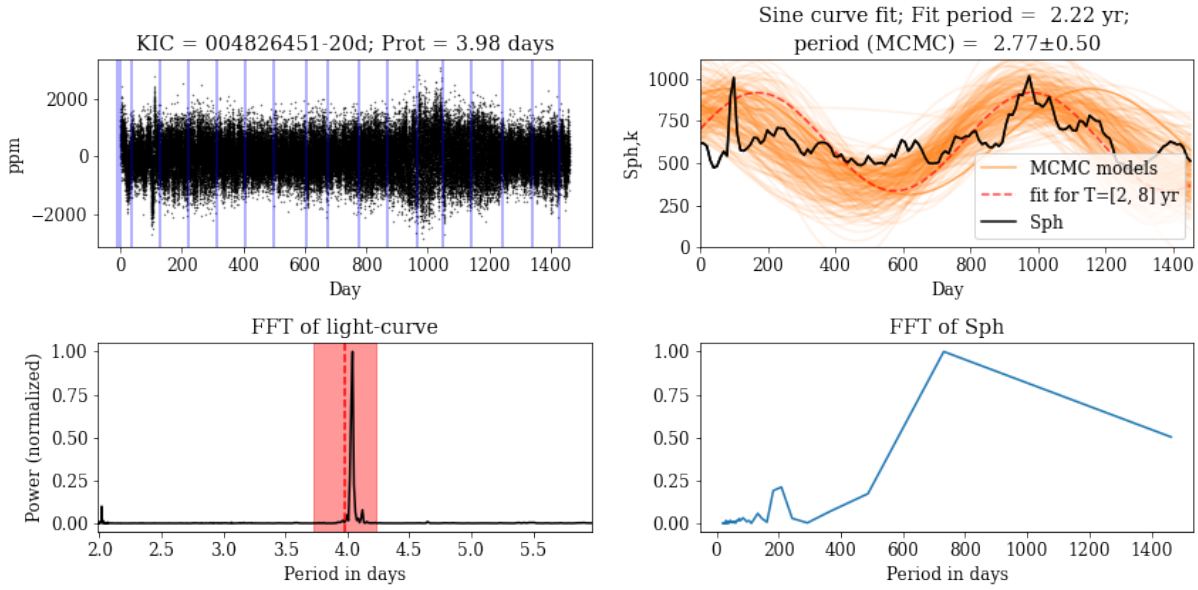

Figure 11. KIC 4826451. Variability cycle observed.

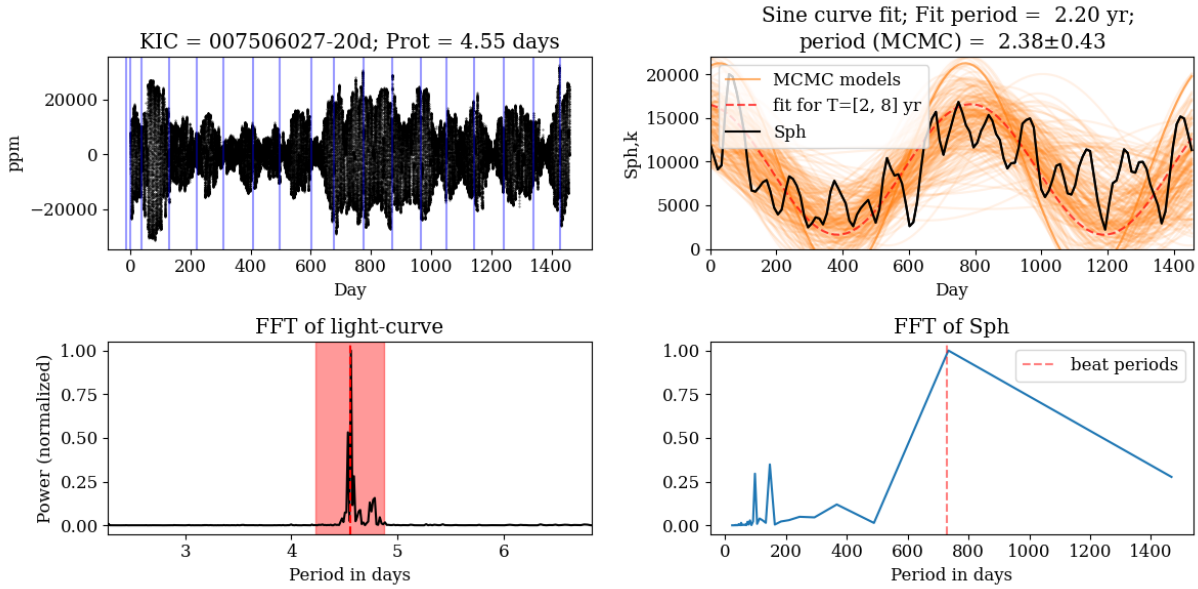

Figure 12. KIC 7506027. Beating of frequencies suspected.

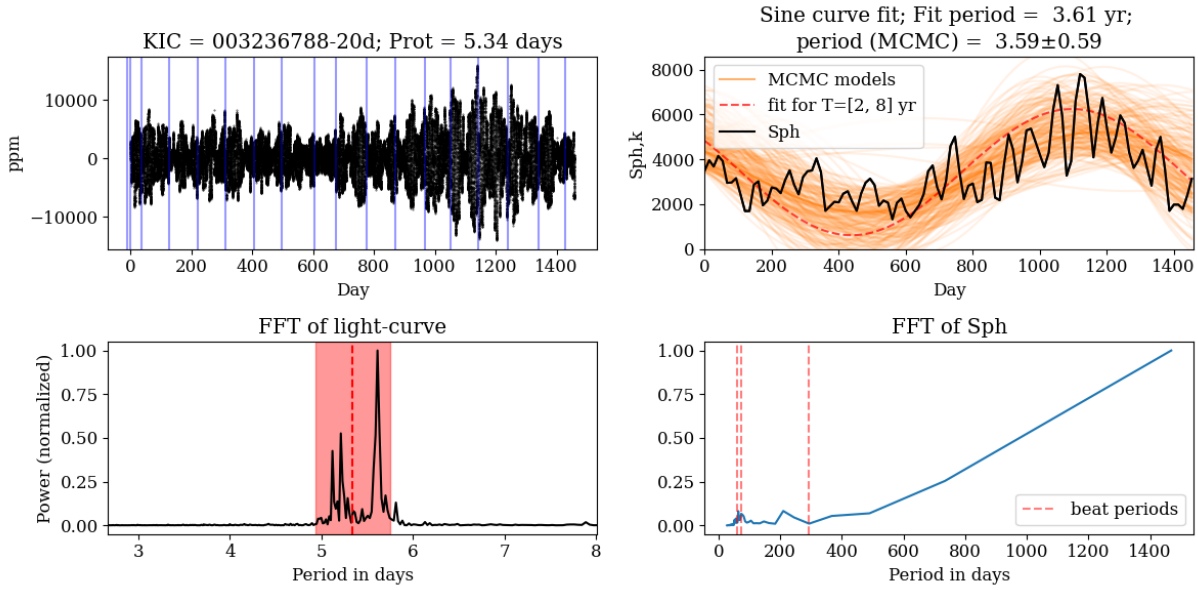

Figure 13. KIC 3236788. Possibility of both activity cycle as well as beating.